CATALYTIC PYROLYSIS OF WASTE TIRE USING NOBLE METALS-SUPPORTED HMOR CATALYSTS

Nguyen Anh Dung
Hanoi University of Mining and Geology
Email: nguyenanhdung@humg.edu.vn

Summary

The catalytic pyrolysis of waste tire over bifunctional catalysts, based on noble metals (Pt, Ru, Re, Rh) supported on HMOR zeolite, was investigated in a semi-batch reactor. The prepared catalysts were characterised by H_2-chemisorption, TPR, TPD of H_2 and NH_3, XRD, N_2-adsorption/desorption and ICP, whereas the spent catalysts were analysed by TPO and XRF. The pyrolysis results indicated an important increase in the yield of gaseous product at the expense of liquid yield when the bifunctional catalysts were introduced. Moreover, the contents of polycyclic and polar-aromatics decreased drastically for all prepared catalysts; and, the reduction of aromatics was more pronounced for poly- and polar-aromatics than for di-aromatics. As a consequence, the derived oils were much lighter and contained high concentration of saturates. The catalytic activity of the studied catalysts for light oil production as well as aromatic reduction can be summarised as followed: Ru/HMOR > Rh/HMOR > Pt/HMOR >> Re/HMOR. Additionally, the catalytic activity under the studied conditions for the current catalysts was independent on the metal dispersion as well as the total concentration of acid sites, but dependent on the intrinsic nature of the metal used. The best performance of Ru catalyst was found to relate to its highest sulfur tolerance and coke resistance.

Key words: *Pyrolysis, waste tire, bifunctional catalyst, Ru, Re, Rh, Pt, MOR.*

1. Introduction

Tire pyrolysis essentially produces a carbonised char, condensable oil and a gas fraction. Gas fraction has been reported to have high calorific value [1], and high hydrogen content [2 - 4], whereas the tire-derived oil was shown to be similar, to a certain extent, to the commercial petroleum naphtha [5]. However, the high concentration of aromatic hydrocarbons (HCs) [5 - 7], especially polycyclic HCs (PAHs), has limited its application as a fuel since a higher smoke, hydrocarbon (HC) and CO emissions were recorded when pyrolysis oil was used in an engine [8]. Our previous study [9], a first step in the attempts to study the possibility of fuel production from waste tire, has shown that the mordenite-catalysed pyrolysis of waste tire produced the oil having high selectivity toward gasoline, kerosene and gas oil fractions. However, a relatively high amount of polycyclic aromatics and polar-aromatics still existed in the oil.

Bifunctional catalysts with both metal and acid functions are extensively studied for the reduction of aromatics in fuels [10 - 13]. Castano et al. studied the aromatics reduction of pyrolysis gasoline over HY-supported catalysts using Pt, Pd, Ir and Ni, and reported that Ir-catalyst was the most effective among the studied catalysts due to its greater metal dispersion, stronger acidity, hydrogen adsorption capacity and metal surface exposure [14]... Meanwhile, Albertazzi et al. investigated the hydrogenation of naphthalene of various metals (Rh, Pd, Pt, Ru, Ir)-supported catalysts and found that the catalytic activity of Rh and Pd-catalysts is higher than that of Ir, Ru, Pt-based catalysts [15].

The aim of this work is to investigate the catalytic activity of noble metals (Ru, Pt, Re, Rh) supported on HMOR catalysts for waste tire pyrolysis. The influences of various noble metal-based catalysts on the nature and yield of products, particularly the pyrolytic oil will be discussed in relation with the catalyst characterisation results.

2. Experiments

2.1. Catalyst preparation

Mordenite (MOR, H-form, SiO_2/Al_2O_3 mole ratio = 19, surface area (BET) = 380m^2/g) zeolite (TOSOH, Singapore) was first calcined in air at 500^{o}C for 3 hours. Then, it was loaded with noble metals, Ru ($RuCl_3$, FLUKA), Rh ($Rh(NO_3)_3$, ALDRICH), Re ($ReCl_3$, FLUKA), Pt ($Pt(NO_3)_3$, FLUKA), using the incipient wetness impregnation technique to obtain 1%wt noble metal-supported catalysts. Then, the samples were dried in the oven at 110^{o}C for 3 hours followed by calcination in a flow of air at 500^{o}C for 3 hours. Next, they were pelletised, ground, and then sieved to specific particle sizes of 400 - 425µm. Prior to the catalytic activity measurement, the catalysts were reduced at 400^{o}C by H_2 for 3 hours.

2.2. Catalyst characterisation

The composition of the prepared catalysts was determined by Inductively Coupled Plasma (ICP) technique using a Perkin Elmer Optima 4300 PV machine after the dissolution of the catalysts using HF solution. The surface area (BET) and pore volume (B.J.H) of the prepared

samples were characterised by N_2 physical adsorption using the Sorptomatic 2900 equipment. XRD patterns were obtained using the Riguku D/Max 2200H using CuKα small radiation, and operated at 40KV and 30mA. The catalyst samples were scanned from 5 to 60 degrees (2θ/θ) with a scanning speed of 5°/min.

Hydrogen chemisorption was carried out using a conventional laboratory made-up system equipped with a TCD detector. Prior to performing the chemisorption at room temperature, an approximate 50mg of reduced sample was pretreated in helium at 150°C for 0.5 hour. Dispersion data was calculated by assuming a stoichiometry H/Ru = 1 [13]. Temperature-programmed desorption (TPD) using NH_3 was conducted in a TPD/TPR Micromeritics 2900 apparatus. Approximately 0.1g of sample was first pretreated in He at 150°C for 30 minutes. Then, the system was cooled to 100°C, and the NH_3 adsorption was performed using NH_3/N_2 for 1.5 hours followed by the introduction of He to remove the physically adsorbed NH_3 for 30 minutes at 100°C. Finally, the system was cooled to 50°C, and then the temperature program desorption was started from 50°C to 600°C with a heating rate of 5°C.min^{-1}. For Temperature-programmed reduction (TPR) using hydrogen, the calcined sample was heated to 150°C and kept at this temperature for 1 hour under the flow of helium to remove water and other contaminants. TPR profiles were recorded with a temperature program from room temperature to 700°C (10°C/min). TPD-H_2 was conducted using the same Micromeritics apparatus. The reduced sample was pretreated by helium flow at 150°C and then cooled to room temperature. H_2 adsorption was performed at room temperature for 0.5 hour using UHP H_2 followed by flushing with helium at the same temperature for another 0.5 hour. The TPD-H_2 was performed from room temperature to 600°C at a rate of 10°C/min under helium flow. The amount of desorbed hydrogen was monitored by a TCD. Temperature-programmed oxidation (TPO) was performed using the apparatus for TPR from room temperature to 900°C (10°C.min^{-1}), and the final temperature was held for 30 minutes. The amount of coke was then determined from the area under the curve and calculated by the software equipped with the machine. The sulfur contents in the spent catalysts were determined by X-ray fluorescence (XRF) spectrometer, Philips PW2400. The catalyst characterisation was done in the Lab at the Petroleum and Petrochemical College, Chulalongkorn University.

2.3. Pyrolysis of waste tire

A used passenger car tire for pyrolysis has a lifetime of 50,000km. The tire was shreaded and crumbed to produce a size range of 0.5 - 1.4mm. The granulated sample was sieved, and the portion with 0.5 - 0.6mm size (30 mesh) was selected for testing.

The detail of pyrolysis process was described elsewhere [9]. Briefly, a tire sample was pyrolysed in the lower zone of the reactor (500°C), and then the evolved product was carried to the upper zone packed with a catalyst (350°C). The obtained product was next passed through a condensing system to separate incondensable compounds from the liquid product. The gas product was stored in a gas bag. The solid and liquid products were weighed to determine the prod uct distribution. The amount of gas was then determined by mass balance. The gaseous product was analysed by a GC equipped with an FID. Prior to being analysed, the liquid product was dissolved in n-pentane to precipitate asphaltenes. The obtained maltenes was analysed by liquid adsorption chromatography [16]. As a consequence, saturated hydrocarbons, mono-, di-, poly- and polar-aromatics in the maltenes were fractionated. Finally, a SIMDIST GC was used to analyse the obtained maltene and hydrocarbon fractions according to the ASTM D2887 method to determine the simulated true boiling point curves. The petroleum fractions were then cut based on their boiling point, including naphtha (< 200°C), kerosene (200°C-250°C), gas oil (250°C - 370°C) and residue (> 370°C).

3. Results and discussion

3.1. Catalyst Characterisation

The amounts of metal loaded on each sample determined by ICP are presented in Table 1. Accordingly, the true numbers were very close to the targeted values. Figure 1 shows the diffraction patterns of the reduced catalysts and HMOR support. Compared to the bare HMOR zeolite, the bifunctional catalysts showed a slight decrease in crystallinity, as deduced from the intensity of peaks at 2θ of 19.76°, 22.46°, 25.76°. However, the peaks corresponding to the metal species were hard to detect, possibly because of the amount of metal loaded was below the detectable range of the machine.

Several structure properties of the prepared catalysts obtained from N_2 adsorption/desorption analysis are also shown in Table 1. The incorporation of noble metal decreased both surface area and pore volume of the

parent zeolite support. And, all the prepared catalysts had comparable surface area and pore volumes.

Metal dispersion determined by H_2-chemisorption is also given in Table 1. It can be seen that there existed small difference between the metal dispersion among all the prepared samples. However, the order of metal dispersion can be summarised as followed: Pt/HMOR > Re/HMOR >Ru/HMOR > Rh/HMOR. In addition, the average metallic particle size in all catalysts was in the range of 2.5nm to 4nm, which was much larger than the pore diameter of the main channel of HMOR zeolite. This, together with the decrease in both surface area and pore volume of the parent zeolite after incorporation of metal, suggested the occurrence of pore blockage and/or the diffusion of noble metal into the zeolite channels.

The acid site strength and concentration in the reduced M/HMOR were revealed by TPD of ammonia and the obtained results are presented in Figure 2. In a good agreement with the TPD-NH_3 study by [17], the ammonia desorption curve of HMOR showed two desorption peaks. The first one located at around 200°C, and the second one peaked at around 540°C, which corresponded to the weak and strong acid sites, respectively. And one should be noted that the weaker acid sites were located closer to the surface, whereas the strong acid sites were located in the deepest part of the zeolite structure [14]. From the figure, obviously the incorporation of noble metals led to a reduction in the intensity of desorption peaks, particularly the peak corresponding to the strong acid sites for all sample. This effect is because a fraction of -OH groups was eliminated by reaction with the metal salt precursors during catalyst preparation and/or the blockage of metal particle decreasing the accessible acid sites, particularly the ones inside the zeolite channels. And the order of total acid site concentration for noble metal-supported catalysts was as follow: Ru/HMOR > Pt/HMOR > Re/HMOR > Rh/HMOR. In the TPD-NH_3 spectra of Rh and Pt catalysts, the number of strong acid sites decreased drastically, suggesting the diffusion of these metal into the zeolite channels, or in other words, higher metal dispersion, which was in good agreement with H_2-chemisorption and N_2-adsorption/desorption results. Surprising us was the TPD-NH_3 profile of the Ru/HMOR, in which a new peak at around 280°C was observed at the temperature in the range corresponding to weak acid sites (Figure 2). This new peak can be attributed to ruthenium clusters since this metal was reported to have high tendency to adsorb ammonia [12] and/or the interaction between metal and support for Ru-based catalyst [18].

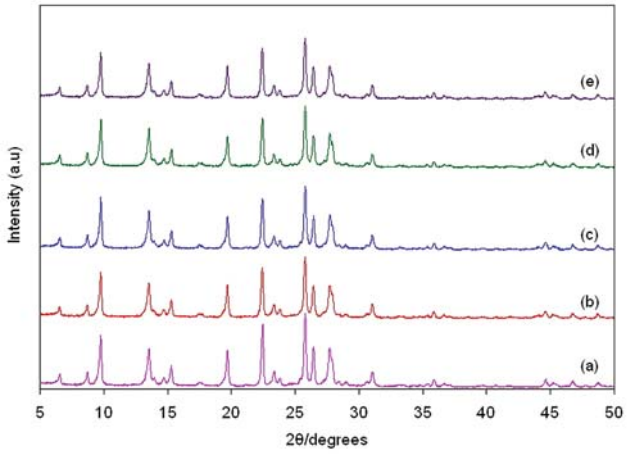

Figure 1. XRD patterns of (a) HMOR, (b) Ru/HMOR, (c) Rh/HMOR, (d) Re/HMOR, and (e) Pt/HMOR

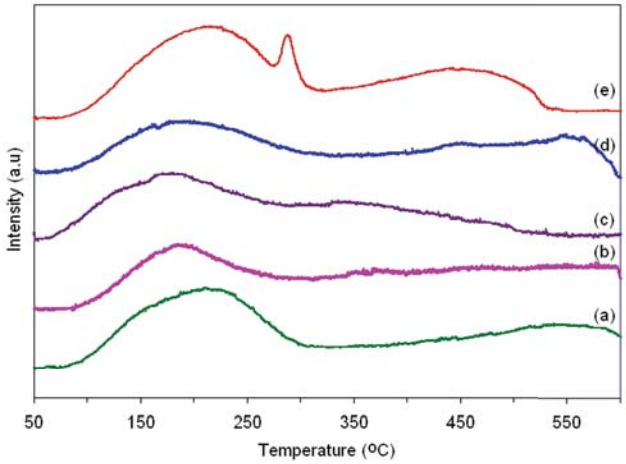

Figure 2. TPD-NH_3 profiles of (a) HMOR, (b) Pt/HMOR, (c) Rh/HMOR, (d) Re/HMOR, and (e) Ru/HMOR

Table 1. Physical and chemical properties of the studied catalysts

Catalyst	M[1] %wt	Dispersion (%)	Surface area ($m^2.g^{-1}$)	Pore volume ($cm^3.g^{-1}$)	Asphaltenes ($g.g^{-1}$ oil)	Coke (% wt)
HMOR	-	-	372.5 ± 9.3	0.231		14.7
Pt/HMOR	0.94	30.8	359.8	0.208	0.000494	21.3
Re/HMOR	0.97	35.4	350.5	0.212	0.000654	29.7
Rh/HMOR	1.02	27.3	352.7	0.217	0.000387	20.8
Ru/HMOR	0.98	21.1	354.9	0.204	0.000309	16.4

[1]*Metal content in % weight (%wt) in the prepared catalyst*

Temperature-programmed reduction is a powerful technique to study the reduction behavior of oxide phases or salts, as well as providing information regarding the degree of interaction between metal and support. Mordenite is comprised of two channel types: (i) larger channel, also called main channel, accessible through twelve member oxygen rings with an opening of 7.0 Å x 6.5 Å, and (ii) smaller channels, often referred to as side-pockets, which include eight member oxygen rings with 3.4 Å x 4.8 Å [19]. Thus, hydrogen with a kinetic diameter of 0.24 nm can enter the inner zeolite structure and the reduction of metal oxides/salts may occur somewhere on the zeolite surface, in the zeolite channels or in the side-pockets [10]. Another important outcome of TPR analysis, therefore, is the location of species in the zeolite. The TPR profiles of all prepared catalysts are shown in Figure 3.

As expected, the TPR profile of the HMOR zeolite showed no peaks. The profile of Rh catalyst showed the two overlapping peaks, maxima at 110°C and 135°C

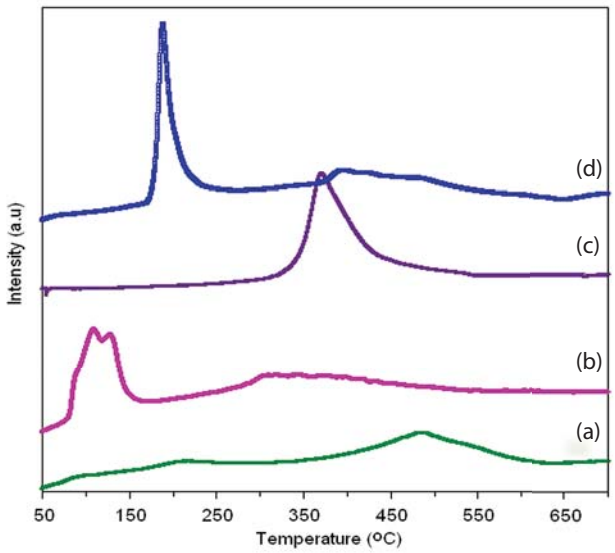

Figure 3. *TPR-H_2 profiles of (a) Pt/HMOR, (b) Rh/HMOR, (c) Re/HMOR, and (d) Ru/HMOR*

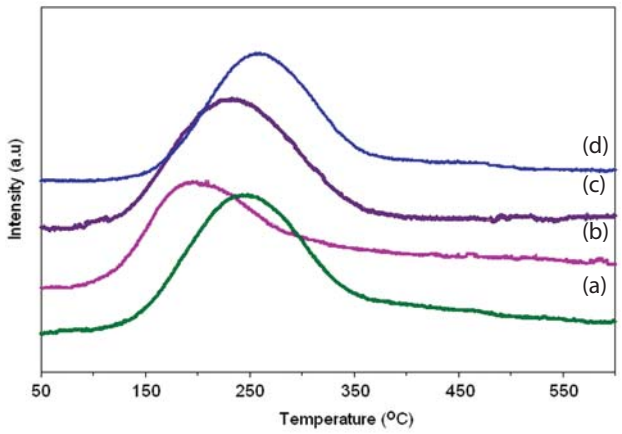

Figure 4. *TPD-H_2 profiles of (a) Pt/HMOR, (b) Rh/HMOR, (c) Re/HMOR, and (d) Ru/HMOR*

that can be attributed to the reduction of Rh(3) in two different environment [20]. These might not be necessary two different electronic states but possibly by Rh_2O_3 with different metal particle sizes, which interact in a different way with the support [20]. Another very broad and low intense peak was also observed at around 350°C in the H_2-consumption curve of Rh-catalyst, suggesting the presence of rhodium species in a more difficult for reduction environment. The TPR result of Pt/HMOR catalyst showed a unique, very broad peak with a maximum occurring at around 498°C. The broad peak suggested the reduction of platinum species located at different environments. Taking into account XRD measurements (Figure 1) and the study of Castano et al. [14], this peak can be ascribed to the reduction of Pt(2) located in the main channel and/or the side-pockets in the zeolite. The hydrogen consumption curve of Re catalyst showed a unique, fairly broad peak at approximate 370°C. The widening of the peak was possibly due to the reduction of rhenium species located in different environments. The Ru/HMOR exhibited a main peak centered at about 198°C. The very intense peak was possibly due to the reduction of Ru(3) poorly dispersed on the surface of the zeolite [21]. The profile also showed a small and ill-defined band of hydrogen consumption between 350°C and 450°C which could correspond to a small amount of ruthenium oxide or oxychloride formed by the exposition and drying in air during catalyst preparation [12].

Figure 4 depicts the TPD-H_2 profiles of all prepared catalysts. Accordingly, TPD profile of the bared zeolite support showed no peak. And all profiles exhibited a unique peak located at temperatures lower than 350°C corresponding to the desorption of hydrogen that chemically adsorbed on the surface of the metallic particles. Considering the intensity of the peak, which is the indication of the hydrogen adsorption on the metallic sites, the observed trend was: Re > Pt > Ru > Rh. This result was in a good agreement with the H_2-chemisorption analysis.

All TPO profiles of the spent catalysts had two peaks (not shown here). The first one located at around 350°C is most likely due to the oxidation of adsorbed hydrocarbon species, which could be formed from condensed polycyclic compounds [22]. And the peak at basically 500 - 600°C might be attributed to the oxidation of deposited carbon species [23]. The quantitative analysis calculated the temperatures of 250°C - 800°C is shown in Table 1. Generally, the order of the amount of coke on the spent catalysts is Re > Rh Pt > Ru.

3.2. Pyrolysis products

3.2.1. Product yields

Figure 5 shows the product distribution, i.e. yield of gas, liquid and solid product, with all catalysts prepared. It can be seen that in the non-catalytic pyrolysis, the yields (%wt) of solid, liquid and gas were approximate 47, 42 and 11, respectively. The solid product was mainly carbonaceous material and therefore, as expected, the yield of solid obtained from all runs was similar. This is attributed to the fact that the pyrolysis conditions were kept constant and the tire was reported to be completely decomposed at 500°C [9].

The presence of catalysts strongly influenced the yield of gas and liquid products. Generally, the use of noble metal supported catalysts increased the gas yield, and the order of gas production was Ru > Pt > Rh > Re > none. It is well known that the products obtained from waste tire pyrolysis contain high concentration of aromatics [5 - 7]. In addition, the catalytic cracking of aromatics should require in a first step the hydrogenation of the aromatic ring over metallic clusters, producing (partial) hydrogenated compounds, which rapidly undergo cracking and/or ring-opening on the acid sites. Meanwhile, all the noble metals used in this study have been reported to exhibit good hydrogenation activity, particularly for the hydrogenation of aromatics and/or desulfurisation [14, 15]. Therefore, a higher conversion of hydrocarbons, especially the aromatics can be achieved with noble metal-supported catalysts. Consequently, the yield of gaseous product increased, whereas that of oil fell off in this paper, when noble metal-supported catalysts were used. The high activity of the noble metal-supported catalysts also led to a drastic asphaltene reduction, as shown in Table 1.

3.2.2. Petroleum fractions

The influences of various noble metal-based catalysts on the petroleum fractions of the derived oils were illustrated in Figure 6. It can be seen that the bifunctional catalysts strongly influenced the contents of petroleum fractions in the oils. And different noble metal-supported catalysts produced oil with different petroleum cuts.

In the non-catalytic oil, although the content of naphtha was the highest (~30%), but there existed a high portion of hydrocarbons distributed in the heavy fractions like residues, gas oil. The treatment of noble metal-supported catalyst led to a shift of hydrocarbons from heavy fractions toward lighter fractions, particularly naphtha, indicating that lighter oils were produced. The high activity of noble metal-supported catalysts for light oil production, again, can be attributed to their bifunctionalities, as mentioned earlier. In general, the order of naphtha production (Figure 6) for different metals was as follow: Ru > Pt > Rh > Re. This order was similar to the order of catalytic activity for conversion of waste tire to gaseous product (Figure 5). However, it should be noted that the activity for naphtha production of Re/HMOR was lower than that of only the zeolite support, HMOR.

3.2.3. Composition of the obtained oil

The oil obtained from non-catalytic pyrolysis contained high concentration of aromatic hydrocarbons, particularly high content of polar-aromatics (~12%wt). Noble metal-supported catalysts significantly affected the compositions of the derived oils, as shown in Figure 7. It can be seen that the contents of saturates and single-ring aromatics increased in accordance with the reduction in both multi-ring aromatic compounds, i.e. di- and poly-aromatics, and polar-aromatics. Moreover, the reduction in poly- and polar-aromatics was more pronounced as compared to the reduction in di-aromatics for all studied catalysts. And the highest activity for aromatic reduction was observed over Ru-based catalyst, meaning that its oil has the highest concentration of saturates, whereas the oil

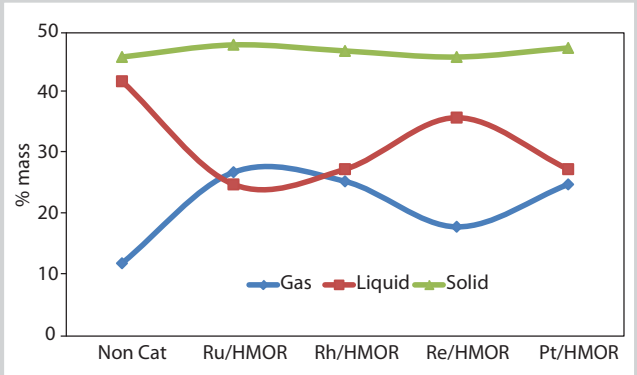

Figure 5. *Yield of pyrolysis products (%wt)*

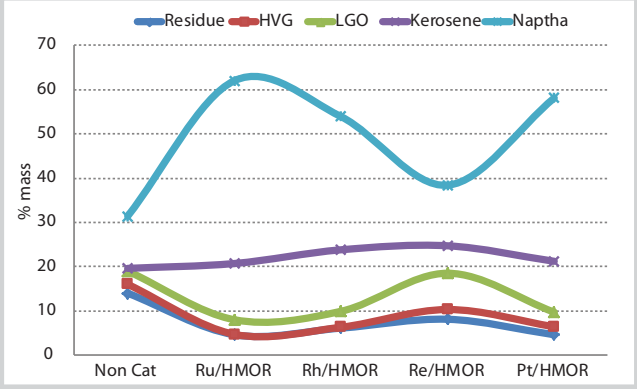

Figure 6. *Petroleum fractions of pyrolysis oils obtained from using various catalysts*

produced over Re/HMOR had the highest concentration of aromatic hydrocarbons. The content of different types of hydrocarbon in oils generated over Rh- and Pt-based catalysts can be comparable. However, Pt-based catalyst produced slightly higher saturates and lower di-aromatics as compared to Rh-supported catalyst.

3.4. Discussion

The complex structure of tire makes it difficult to understand the multi-reactions occurring during pyrolysis. And aromatics are produced and consumed during catalytic pyrolysis of waste tire through different reactions, such as Diels-Alders reaction, aromatisation, condensation, dealkylation, hydrogenation, and cracking, etc [4, 9, 24]. As reported in our previous paper, the use of HMOR decreased the poly- and polar-aromatics content in the derived oil [9]. And compared to the bared zeolite support, the incorporation of noble metal to the zeolite led to a further reduction in the concentration of multi-ring aromatic compounds as well as polar-aromatics, except for Re/HMOR (Figure 7).

Table 2 summarises the kinetic diameters of several aromatics [25]. As such, the main channel of the zeolite support is not accessible for the poly-aromatics but for di-aromatics, to a small extent. Meanwhile, from H2-chemisorption analysis and TPR profiles, a considerable amount of noble metal particles locates outside the zeolite structure. Moreover, for HMOR zeolite, the weak acid sites

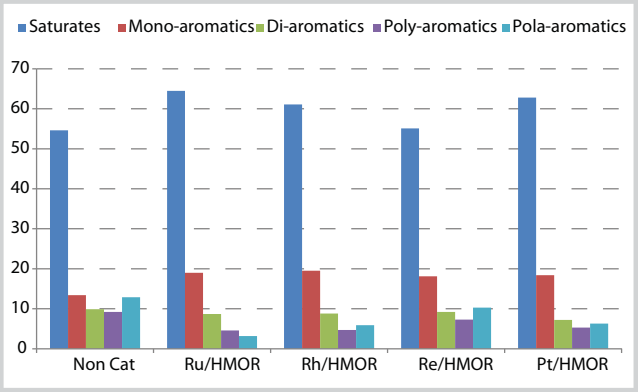

Figure 7. *Compositions of pyrolysis oils obtained from using various catalysts*

Table 2. *The kinetic diameters of several aromatics [23]*

Compound	H/C atomic ratio	Boiling point (°C)	Molecular size (Å)
Alkylbenzenes	1.0 - 1.4	200 - 250	5.0 x 6.8
Naphthalene	1.26	218	6.0 x 7.0
Tetrahydronaphthalene	1.38	206	6.0 x 7.0
Anthracene	0.94	340	6.0 x 9.5
Pyrene	0.63	404	8.5 x 8.5

were mainly located at the outer surface of the zeolite, as revealed from TPD-NH3 analysis. And the amount of weak acid sites accounted for a high portion of the total acid sites in the prepared bifunctional catalysts. Therefore, on the outer surface of the zeolite support there was a high concentration of both metallic and acidic sites that were accessible for the di-, poly- and polar-aromatics trying to enter the zeolite channels. Accordingly, the multi-ring aromatics might be hydrogenated over metallic sites, producing (partial) hydrogenated compounds, which rapidly undergo cracking and/or ring-opening on the acid sites [26]. The presence of noble metal had another advantage in that it can prevent the formation of the polar- and poly-aromatics by converting their precursors followed by cracking over acidic sites [24]. As a consequence, the presence of noble metal promoted the conversion of the heavy compounds like multi-ring aromatic and polar-aromatics to the lighters, thus, producing lighter oil and the oil contains higher concentration of saturates (Figure 6 and Figure 7). The higher reduction of poly-aromatics than di-aromatics can be ascribed to the higher reactive for hydrogenation of the former [27]. However, the high amount of coke (Table 1) that might be generated by the condensation of the polycyclic aromatics [9] and polar-aromatics [24] should not be excluded for the reduction of these compounds in the oil after catalysis treatment.

TPR analysis revealed that the reduction temperatures of Re and Pt supported on HMOR catalysts were, to a certain extent, higher than that used for catalyst reduction during preparation. Therefore, the reduced samples were subjected to analysis by TPR. The complete reduction of all prepared samples was confirmed since the reduced samples did not consume any hydrogen. This effect might be explained by the long reaction time of reduction employed (3 hours, 500°C).

On the other hand, it is well accepted that the metal dispersion strongly influences the catalytic activity of a metal-supported catalyst. And the hydrogenation activity of noble metal-supported catalysts increased with increasing metal dispersion [28]. In this paper, the order of metal dispersion for the prepared catalysts as revealed from H2-chemisorption analysis was: Pt > Re > Ru > Rh. Besides, it has been reported that the cracking reactions over acid sites are dominant compared with hydrogenolysis over metal sites [14]. For the prepared catalysts, the order of total concentration of acid sites as revealed from TPD-NH_3 analysis was: Ru > Pt > Re > Rh.

Considering the catalytic activity for the reduction of multi-ring and polar-aromatics and simultaneously the production of light oil of the prepared catalysts, the order can be summarised as followed: Ru > Pt > Rh > Re. One can see that this order did not match the accessible number of metal or acid sites. Therefore, it is safe to conclude that the metallic nature strongly influences the catalytic activity of the noble metal supported on HMOR catalysts.

As revealed from TPO analysis, the lowest amount of coke was detected on the spent ruthenium catalyst, whereas Re catalyst produced the highest amount of coke [Table 1]. Meanwhile, liquid analysis revealed a considerable amount of polar-aromatics, which were mainly sulfur-containing aromatics [24]. Furthermore, due to the intrinsic structure of HMOR zeolite that has one main channel, once one segment of the channel is block, the whole channel is rendered inactive. Therefore, it is proposed that Re/HMOR displayed the lowest sulfur tolerance, resulting in a very quick deactivation, explaining its poorest catalytic activity performance. In contrast, Ru catalyst showed the best catalytic activity due to its intrinsic nature that gives high sulfur tolerance. Rodriguez-Castellon et al. reported that Ru exhibited a better sulfur tolerance than Pt, Pd or Pd-Pt catalysts due to the low density of states at the Fermi level of this metal [20]. Consequently, the spent catalysts were subject to analysis for their sulfur contents using XRF. Accordingly, the sulfur (%wt) in the Ru, Rh, Pt, Re spent catalysts were 0.78, 1.21, 1.35 and 2.51, respectively. This result confirmed the highest sulfur tolerance of the ruthenium catalyst among the studied samples. Furthermore, sulfur-containing compounds might deactivate the metal-supported catalysts [12] by the strong bonding between the sulfur atoms and metal atoms [23], making the metal sites inactive. It is appreciable that when the metallic function has no proper hydrogenation activity, the unsaturated bonds can not react quickly enough. Moreover, the acid sites generate alkenes and aromatics from β-scission and aromatisation (cyclisation and subsequent hydride transfer), respectively [14]. Furthermore, the high temperature used in this study was, to a certain extent, responsible for favourable aromatisation. That explained the high concentration of aromatics generated over this Re catalyst than over other metal-supported catalysts.

4. Conclusions

The uses of noble metals (Rh, Re, Ru, Pt) supported on HMOR catalysts produced an important increase in the yield of gaseous product at the expense of the oil yield. This effect was attributed to the high activity of the bifunctional catalysts for the conversion of polycyclic and polar-aromatic hydrocarbons into lighter compounds. And the aromatic reduction was more pronounced for poly- and polar-aromatics than for di-aromatics. The polycyclic and polar-aromatic reduction and simultaneously light oil production activities for the current catalysts can be summarised in the order: Ru/HMOR > Rh/HMOR > Pt/HMOR >> Re/HMOR. We found that these activities were independent on the metal dispersion as well as the total acid concentration, but the intrinsic nature of the noble metal used. The best catalytic performance of ruthenium catalyst was ascribed to its metallic nature that exhibited the highest sulfur tolerance, resulting in the least coke formation.

References

1. Mahmood M.Barbooti, Thamer J.Mohamed, Alaa A.Hussain, Falak O.Abas. *Optimization of pyrolysis conditions of scrap tires under inert gas atmosphere.* Journal of Analytical and Applied Pyrolysis. 2004; 72(1): p. 165 - 170.

2. C.Berrueco, E.Esperanza, F.J.Mastral, J.Ceamanos. P.García-Baicaicoa. *Pyrolysis of waste tyres in an atmospheric static-bed batch reactor: Analysis of the gases obtained.* Journal of Analytical and Applied Pyrolysis. 2005; 74(1-2): p. 245 - 253.

3. E.Aylon, R.Murillo, A.Fernandez-Colino, A.Aranda, T.Garcia, M.S.Callen, A.M.Mastral. *Emissions from the combustion of gas-phase products at tyre pyrolysis.* Journal of Analytical and Applied Pyrolysis. 2007; 79(1-2): p. 210 - 214.

4. Paul T.Williams, David T.Taylor. *Aromatization of tyre pyrolysis oil to yield polycyclic aromatic hydrocarbons.* Fuel. 1993; 72(11): p. 1469 - 1474.

5. B.Benallal, C.Roy, C.Pakdel, S.Chabot, M.A.Poirier. *Characterization of pyrolytic light naphtha from vacuum pyrolysis of used tyres comparison with petroleum naphtha*. Fuel. 1995; 74: p. 1589 - 1594.

6. Adrian M.Cunliffe, Paul T.Williams. *Composition of oils derived from the batch pyrolysis of tyres*. Journal of Analytical and Applied Pyrolysis. 1998; 44(2): p. 131 - 152.

7. Paul T.Williams, Richard P.Bottrill. *Sulfur-polycyclic aromatic hydrocarbons in tyre pyrolysis oil.* Fuel. 1995; 74(5): p. 736 - 742.

8. S.Murugan, M.C.Ramaswamy, G.Nagarajan. *Assessment of pyrolysis oil as an energy source for diesel*

engines. Fuel Processing Technology. 2009; 90(1): p. 67 - 74.

9. Nguyen Anh Dung, A.Mhodmonthin, S.Wongkasemjit, S.Jitkarnka. *Effects of ITQ-21 and ITQ24 as zeolite additives on the oil products obtained from the catalytic pyrolysis of waste tire.* Journal of Analytical and Applied Pyrolysis. 2009; 85(1-2): p.338 - 344.

10. Alois Lugstein, Andreas Jentys, Hannelore Vinek. *Hydroisomerization and cracking of n-octane and C8 isomers on Ni-containing zeolites.* Applied Catalysis A: General. 1999; 176(1): p.119 - 128.

11. M.A.Ali, T.Kimura, Y.Suzuki, M.A.Al-Saleh, H.Hamid, T.Inui. *Hydrogen Spillover phenomenon in noble metal modified clay-based hydrocracking catalysts.* Applied Catalysis A: General. 2002; 277(1-2): p. 63 - 72.

12. D.Eliche-Quesada, Meria-Robles. E.Rodriguez-Castellon, A.Jimenez-Lopez. *Influence of the incorporation of palladium on Ru/MCM hydrotreating catalysts.* Applied Catalysis B: Environmental. 2006; 65(1-2): p.118 - 126.

13. D.Eliche-Quesada, M.I.Macias-Ortiz, J.Jimenez-Jimenez, E.Rodriguez-Castellon, J.Jimenez-Lopez. *Catalysts based on Ru/mesoporous phosphate heterostructures (PPH) for hydrotreating of aromatic hydrocarbons*. Journal of Molecular Catalysis A: Chemical. 2006; 225(1-2): p. 41 - 48.

14. P.Castano, B.Pawelec, J.L.G.Fierro, J.M.Arandes, J.Bilbao. *Aromatics reduction of pyrolysis gasoline (PyGas) over HY-supported transition metal catalysts.* Applied Catalysis A: General. 2006; 315: p. 101 - 113.

15. S.Albertazzi, R.Ganzerla, C.Gobbi, M.Lenarda, M.Mandreoli, E.Salatelli, P.Savini, L.A.Storaro. Vaccari, *Hydrogenation of naphthalene on noble-metal-containing mesoporous MCM-41 aluminosilicates.* Journal of Molecular Catalysis A: Chemical. 2003; 200: p. 261 - 270.

16. Gustav Sebor, Josef Blazek, Muaz Fathi Nemer. *Optimization of the preparative separation of petroleum maltenes by liquid adsorption chromatography.* Journal of Chromatography A. 1999; 847(1-2): p. 323 - 330.

17. Nitin Labhsetwar, H.Minmino, M.Mukherjee, T.Mitsuhashi, S.Rayalu, M.Dhakad, H.Haneda, J.Subrt, S.Devotta. *Catalytic properties of Ru-mordenite for NO reduction.* Journal of Molecular Catalysis A: Chemical. 2007; 261(2): p. 213 - 217.

18. V.M.Akhmedov, S.H.Al-Khowaiter. *Hydroconversion of C5-C8 alkanes over Zr-containing supported catalysts prepared by metal vapor method*. Applied Catalysis A: General. 2000; 197: p. 201 - 212.

19. J.L.de Macedo, S.C.L.Dias, J.A.Dias. *Multiple adsorption process description of zeolite mordenite acidity.* Microporous and Mesoporous Materials. 2004; 72(1-3): p. 119 - 125.

20. E.Rodriguez-Castellon, J.Mérida-Robles, L.Díaz, P.Maireles-Torres, D.J.Jones, J.Rozière, A.Jiménez-López. *Hydrogenation and ring opening of tetralin on noble metal supported on zirconium doped mesoporous silica catalysts.* Applied Catalysis A: General, 2004; 260(1): p. 9 -18.

21. D.Eliche-Quesada, E.Rodríguez-Castellon, A.Jiménez-Lopez. *Hydrodesulfurization activity over supported sulfided ruthenium catalysts: Influence of the support*. Microporous and Mesoporous Material. 2007; 99, p. 268 - 278.

22. J.Zheng, M.Guo, C.Song. *Characterization of Pd catalysts supported on USY zeolites with different* SiO_2/Al_2O_3 *ratios for the hydrogenation of naphthalene in the presence of benzothiophene.* Fuel Processing Technology. 2008; 89: p. 467 - 474.

23. C.Naccache, M.Primet, M.V.Mathieu. *Study of hydrogen and carbon monoxide interactions with palladium-Y zeolite by ESR and IR Spectroscopy.* Advances in Chemistry Series. 1973; 121: p. 266 - 280.

24. Nguyen Anh Dung, Sujitra Wongkasemjit, Sirirat Jitkarnka. *Effects of pyrolysis temperature and Pt-loaded catalysts on polar-aromatic content in tire-derived oil*. Applied Catalysis B: Environmental. 2009; 91, p. 300 - 307.

25. Tseng-Chang Tsai. *Reactivation of acidic sites in mordenite used in toluene disporportionation.* Applied Catalysis A: General. 2006; 301: p. 292 - 298.

26. Nguyen Anh Dung, Walairat Tanglumlert, Sujitra Wongkasemjit, Sirirat Jitkarnka. *Roles of ruthenium on catalytic pyrolysis of waste tire and the changes of its activity upon the rate of calcinations*. Journal of Analytical and Applied Pyrolysis. 2010; 87: p. 256 - 262.

27. A.Corma, A.Martinez, V.Martinez-Soria. *Hydrogenation of aromatics in diesel.* Journal of Catalysis. 1997; 169(2): p. 480 - 489.

28. D.Eliche-Quesada, J.M.Merida-Robles, E.Rodriguez-Castellon, A.Jimenez-Lopez. *Ru, Os and Ru-Os supported on mesoporous silica doped with zirconium as mild thio-tolerant catalysts in the hydrogenation and hydrogenolysis/hydrocracking of tetralin.* Applied Catalysis A: General. 2005; 279(1-2): p. 209 - 221.